Effect of high temperatures on sandstone - a computed tomography scan study

Yang Lintao, PhD
Nottingham Centre for Geomechanics, University of Nottingham, Nottingham, UK
Alec M. Marshall, PhD
Nottingham Centre for Geomechanics, University of Nottingham, Nottingham, UK
Dariusz Wanatowski, PhD
Faculty of Science and Engineering, University of Nottingham, Ningbo, China
Rod Stace, PhD
Nottingham Centre for Geomechanics, University of Nottingham, Nottingham, UK
Thushan Ekneligoda, PhD
Nottingham Centre for Geomechanics, University of Nottingham, Nottingham, UK
* Alec M. Marshall, PhD
University of Nottingham, Department of Civil Engineering, Room B59 Coates Building, University Park, Nottingham UK, NG7 2RD
Email: Alec.Marshall@nottingham.ac.uk
Tel.: +44 (0)115 951 3908

The impact of high temperatures on rocks is a topic of growing importance in geotechnical engineering because of its relevance to applications such as underground nuclear fuel storage, geothermal energy resource exploration, and underground coal gasification (UCG). This paper presents results from tests performed on samples of sandstone treated to a range of temperatures between 20 and 1000 °C. Sandstone samples obtained from underground coal gasification (UCG) trial sites in Poland were selected for the tests. Multistage triaxial tests were used to determine the mechanical properties of the samples. X-ray diffraction (XRD) and thermal analyses (TA) were performed to investigate the changes in the physical and chemical properties of the samples under increasing temperature. Micro-computed gomography analyses were carried out on selected samples in order to reveal the microstructural changes that take place as a result of the heating process. 3D characterization of the sample porosity and pore size distribution were performed to obtain a quantitative comparison between samples subjected to different temperature treatments. The relationship between micro-structure and macro-mechanical characteristics of sandstone at high temperature is discussed. The results illustrate that the mechanical properties of sandstone are closely related to alterations of microstructure that result from increased temperatures.

1. Introduction

The effect of high temperature on the thermo-mechanical response of rocks is important for several engineering applications, including underground nuclear waste storage, geothermal energy resource exploration, and underground coal gasification (UCG). Generally, the scope of high temperature ranges from normal temperatures (10-50 °C) to extreme temperatures (1000-1500 °C). Under the influence of high temperatures, the mechanical properties of rock can change significantly and this influences the deformation and stability of rock structures. Temperature dependent mechanical parameters such as strength, elastic modulus and Poisson's ratio are the basic parameters relevant to deep underground excavation support design and stability analyses. Hence, the impact of high temperatures on rocks is considered as an important topic in rock mechanics.

The deformation mechanisms and failure criteria of different types of rocks at high temperatures has been studied by various researchers (Stesky et al. 1974; Heuze 1983; Rao et al. 2007; Wan et al. 2009; Zhang et al. 2009; Chen et al. 2012; Ranjith et al. 2012; Brotóns et al. 2013; Wu et al. 2013; Liu et al. 2013; Zhang et al. 2014) and it has generally been shown that high temperature has a significant effect on the mechanical properties of rocks. However, the extent of the effect has been shown to vary for different types of rock, depending on

factors such as mineral composition, porosity, density, and presence of cracks. The strength of crystalline and sedimentary rocks have been found to increase when heated up to 800 °C, but decrease rapidly upon further heating (i.e. >800 °C) (Ranjith et al. 2012; Chen et al. 2012; Wu et al. 2013; Zhang et al. 2014; Mao et al. 2009). For sedimentary rocks, a decrease in strength has been observed for moderate levels of temperature increase (<200 °C), with less significant strength loss occurring at higher (>400 °C) temperatures (Zhang et al. 2009; Mao et al. 2009). The temperature range of 400 to 600 °C has been observed to be the most significant in terms of changing rock property. The rocks have also been noted to respond in a brittle manner up to temperatures between 400-600 °C, and be more ductile for higher temperatures.

In the natural state, the rock microstructure commonly displays a complex mixture of minerals, bonding matrix, composite microcrack systems and pores, which are formed during various natural processes (Vollbrecht et al. 1991). It is believed that the effects of high temperature on the mechanical properties of rocks are closely related to their mineral composition and microstructure features. However, due to lack of effective techniques for microscopic observation, the deformation-failure mechanisms of rocks under high temperature were not adequately addressed at the microscale in earlier studies. During the past few decades, with the increased diversity and precision of experimental methods and techniques, researchers have been able to explore the microstructure of rocks through various advanced laboratory techniques. Using a micro-photometer, Zhang et al. (2005, 2007) investigated the characteristics of micro thermal crack development of sandstone samples when heated up to 1350 °C. The results showed that the microcracks of the sandstone sample increased dramatically after 150 °C and then gradually stabilized before a second peak at 810 °C. Thermal melting and decomposition happens to part of the sandstone minerals upon further heating up to 1000 °C. Based on scanning electron microscopy (SEM) observation and mineral component analysis of limestone after high temperature treatment, Liu et al. (2008) showed that the mineral compositions of the sample changed continuously in the temperature range of 100-800 °C. The process also included continuous water evaporation, dehydration and phase change of enhydrite. Using X-ray diffractometer (XRD) and SEM, Zhang et al. (2014) analysed the mineral composition and fracture mechanism of high temperature treated mudstone samples after uniaxial compressive loading. The findings demonstrated that extensive intergranular and intragranular cracks were formed when the temperature was raised above 800 °C. Consequently, a significant reduction of the sample strength occurred.

The microscopic observations provide an important approach to gain a fundamental understanding of the internal structure of rocks that is directly responsible for their mechanical characteristics as well as their response to high temperatures. However, most of the micro-studies mentioned above focused mainly on morphological observations on the sample surface and the mineralogical phase analysis in a qualitative manner. Although it is believed that the changes of mechanical properties of rocks under high temperature depend strongly on the evolution of the void network, few investigations have been conducted to investigate the changes in the rock internal pore structure as well as the development of microcracks under high temperature. Micro X-ray Computed Tomography (micro-CT) is a powerful tool for detecting the microscale pore structure with high resolution (voxel sizes down to 1μm or smaller; a voxel is a 3D version of a pixel) compared to the conventional medical X-ray tomography. Micro-CT and image analysis techniques are fast becoming key tools for accurate and non-destructive characterization of the microstructure of many engineering materials such as metal alloys, ceramics, polymers, soils and rocks (Stefaniuk et al., 2014). This paper aims to provide a better understanding of the complex cracking mechanisms and void network evolutions that take place in the rock microstructure under increasing temperature. Experimental results of micro-CT scanning and traditional rock mechanics tests performed on rock samples treated to a range of temperatures between 20 and 1000 °C are presented. Multistage triaxial tests were used to determine the mechanical properties of the samples. X-ray diffraction (XRD) and thermal analyses (TA) were performed to investigate the changes in the physical and chemical properties of the samples under increasing temperature. Micro-CT analyses were performed on selected samples in order to reveal the microstructural changes that take place as a result of the heating process.

2. Materials and methods

2.1 Specimen and preparation

An underground trial of UCG was conducted at the Wieczorek colliery in Poland in 2014. The UCG geo-reactor was located within a coal seam at a depth of 450m. Prior to undertaking gasification, a borehole was drilled in the floor of the roadway above the gasified seam, from which a core measuring approximately 9 m long and 100 mm diameter was obtained. The roof of the roadway was found to contain mainly fine and coarse sandstone. The obtained samples were sub-cored and ends ground flat to obtain specimens measuring approximately 37 mm in diameter and 74 mm in height. Sixteen intact core samples were obtained for testing, as illustrated in Figure 1.

In order to improve the image quality and achieve high-resolution of 2D slice images in micro-CT analysis, a smaller sized sample is preferred. The rock coring machine was used to make two samples with 10 mm diameter and approximately 20 mm height for the CT

scanning. As shown in Figure 2, two representative samples of coarse and fine sandstone were collected from the original core. As the XRD and TA analyses require the testing material to be the finely pulverized powder, samples collected at nearby positions were ground and homogenized in an agate mortar.

2.2 Experimental program

After air drying for two weeks, samples were placed in a Carbolite laboratory chamber furnace for heat treatment, where the rate of the temperature change was set using a built-in temperature controller. Temperature was gradually increased from room temperature to a target temperature at a rate of 5°C/min in order to minimise thermal shock and the development of stress fractures. Samples were kept at the target temperature for a minimum of 12 hours and then allowed to cool gradually back to room temperature. Four pre-treatment temperatures were considered: 20°C (room temperature), 400 °C, 800 °C, and 1000 °C. The 16 core samples was insufficient to enable determination of the failure envelope of the rocks at the four temperature values using conventional triaxial testing. Conventional triaxial testing would require a separate sample to be tested at each confining stress (minimum of 3 stresses) for each temperature. As such, multistage triaxial testing was adopted, which allowed for 2 samples to be tested at each temperature value, as detailed in Table 1. The multistage triaxial test is useful when a limited number of samples are available and enables more consistent strength data by eliminating issues related to sample variation. Multistage triaxial tests were conducted at confining stresses of 0, 6, 9, and 12 MPa. All tests were carried out according to the suggested methods outlined in the International Society of Rock Mechanics (ISRM) guidelines (Brown 1981).

Table 1 presents measurements and percentage changes of volume, mass, and density of the 16 intact samples (note positive values indicate an increase in parameter value). Figure 3(a) and (b) present the volume, mass, and density changes of the coarse and fine sandstone after different temperature treatment (based on averaging values from the 2 samples). For both coarse and fine sandstone, upon heating to 400 °C, not much difference is observed for the parameters when compared to those at 20 °C. When the heat-treating temperature was increased to 800 °C, a significant mass reduction, volume expansion, and porosity rise of the rock occurred. The fine sandstone is noted to exhibit more severe changes than the coarse sandstone. When the temperature was increased further to 1000 °C, the change rate of the parameters decreased; this trend is more obvious for coarse sandstone samples.

2.3 Micro-CT and data processing

The Micro-CT scanning data presented in this paper was gathered using the XRADIA Versa XRM-500 micro-CT system available at the University of Nottingham. It is one of only three systems of its kind currently in the UK. This state-of-the-art system is designed for non-destructive micro tomography with high resolution 3D X-Ray imaging. It enables control over resolution and phase contrast across a wide range of sample sizes to support a diverse range of applications, including: semiconductor, material science, geology and life sciences. Using the system, a CT scan was performed on the prepared rock samples after being subjected to heat treatment of 20, 400, 800, and 1000 °C. In order to obtain comparable imaging data, the same sample was used for CT scanning each time after the sample had been cooled back to room temperature. To acquire a high resolution CT slice image, cylindrical samples as small as possible are needed (Peng et al. 2012). As mentioned in Section 2.1, two representative cylindrical specimens were prepared with 10 mm diameter and approximately 20 mm height. In order to further increase the resolution and save scanning time, the scan was conducted on a sub-volume in the centre of the sample with a dimension of 5 mm diameter and 5 mm height. In total 1,024 images with a pixel size of 5 μm were recorded. For typical fine sandstone, the dominant pore-throat sizes ranges from about 0.1–90 μm (Bloomfield et al. 2001). Therefore, not all the fine sandstone pores could be detected by CT scanning using the current micro-CT system. However, for the purpose of examining pore characteristics of the same sample subjected to different temperature treatment, such a limitation does not have a significant impact on results.

The 2D raw images of the rock sample obtained from the CT scanning were processed with Avizo 9.0, an advanced 3D visualization and analysis software application designed for processing large three-dimensional data sets, principally those produced by X-ray CT. In order to save computation time and enhance visual inspection effects, the image processing and analysis was performed on a subset volume of a 3×3×3 mm cube (600×600×600 voxels). Improving image quality is often necessary to obtain the best results with image analysis. Therefore, in the first step, the Non-Local Means filter (extremely effective on noisy data while preserving edges) was applied for image smoothing and noise reduction. The thresholding process group's pixels lie between an upper and a lower boundary greyscale value. Each group comprising pixels of similar grey scale values is associated, on the basis of the imaging of a known control specimen, with a constituent element of the mixture. Thus the process assigns a specific range of grey values to air voids and other ranges to mixtures of minerals within the rock, thereby allowing the pore structure of the rock to be separated out. The Avizo Interactive Thresholding module which prompts

users to determine the boundary greyscale threshold with a visual feedback was used to transfer the greyscale image into a binary image with only interior pores and exterior materials. In this study, the boundary grey threshold was determined as the average of the greyscales of pores and grains according to the standard approach of CT image processing in ASTM (1992). For comparison purposes, the same value of boundary greyscale was selected as the threshold value that defined a void for analysis of each sample. After thresholding, the resultant 2D slice binary images were then used for the reconstruction of 3D pore structure.

3. Results

3.1 Mechanical testing results

Figure 4 (a)-(d) shows the stress-strain curves obtained from the multistage triaxial tests (confining stresses of 0, 6, 9 and 12 MPa) performed on the coarse and fine sandstone samples. Peak stresses at each confining stress are indicated with cross-marks. The stress-strain data show similar trends at the different confining stress levels with change of heating temperature for the two sandstone types; an initial linear stage, followed by non-linear response, and finally brittle failure (at 12 MPa confining stress). Maximum stress is noted to increase from room temperature to 400 °C, with little change in stiffness. For a preheating temperature of 800 °C, the strength increased again (most notably for the fine sandstone), but with a considerable change in the sample stiffness (larger strains at peak stresses). The maximum stress generally decreased slightly for both samples treated to 1000 °C

Figure 5 presents the data of peak stress against preheating temperature at the four levels of confining stress tested in the multistage triaxial tests (solid black lines/marks = coarse sandstone; dashed red lines/marks = fine sandstone). The solid lines pass through the average of the values at each confining stress. The variation of the peak stresses with increasing temperature are shown to follow similar trends at different confining stresses for the same type of sample. For fine sandstone, the peak stress increases as the preheating temperature increases up to 800 °C and then decreases as the temperature is increased from 800 to 1000 °C. Similar observations from sandstone under high temperature were reported by Ranjith et al. (2012). The coarse sandstone is shown to be less sensitive to the effects of heat treatment compared to the fine sandstone; only relatively small changes of peak stress with increasing preheating temperature are noted for the coarse sandstone.

Figure 6 shows secant Young's modulus (at 50% of the maximum stress at a given level of confining stress) plotted against the preheating temperature at different confining pressures. The fine sandstone is noted to have a higher Young's modulus than the coarse sandstone. The Young's modulus of the fine sandstone (dashed red lines) decreases continuously with increasing preheating temperature, reducing by about 70% at 1000 °C compared to room temperature. A slight increase in Young's modulus (5% ~ 10%) is noted for the coarse sandstone (solid black lines) when the preheating temperature is below 400 °C. Both sandstones experienced a significant reduction of Young's modulus when the preheating treatments increased from 400 to 800 °C, with an average reduction of about 50 % and 40 % for fine and coarse sandstone, respectively. Similar variation patterns of the Young's modulus of sandstone under increasing temperature were reported by Wu et al. (2013).

3.2 XRD and TA results

X-ray diffraction (XRD) is a rapid analytical technique used for phase identification of crystalline material. In order to investigate potential changes in the mineral composition of sandstone with high temperature treatment, XRD analysis was performed on selected samples after different temperature treatment. Both coarse and fine sandstone showed similar types of mineral composition from XRD analysis. As shown in Figure 7, from the diffraction intensity of X-rays at different detection angles, the crystalline phases of the material were identified and represented by lines with different colours. Figure 7 (a) shows that the mineral composition of the sandstone at room temperature mainly consists of quartz, kaolinite, orthoclase and illite. After 800 °C thermal treatment (Figure 7 (b)), the diffraction intensity of quartz, orthoclase and illite remains relatively stable, however kaolinite disappeared. By further heating the sample to 1000 °C, as shown in Figure 7 (c), mullite was formed.

As indicated in the chemical reaction equations:

1. $Al_2O_3 \cdot 2SiO_2 \cdot 2H_2O$ (kaolinite) $\rightarrow Al_2O_3 \cdot 2SiO_2$ (metakaolinite) $+ 2H_2O\uparrow$

2. $Al_2O_3 \cdot 2SiO_2$ (metakaolinite) $\rightarrow SiAl_2O_4$ (spinel) $+ SiO_2$ (amorphous)

3. $SiAl_2O_4$ (spinel) $+ SiO_2$ (amorphous) $\rightarrow 1/3$ $(3Al_2O_3 \cdot 2SiO_2)$ (mullite) $+ 4/3SiO_2$ (amorphous)

Kaolinite undergoes significant changes in its structure when heated up to high temperatures. Dehydration of kaolinite begins at temperatures between 500 and 600 °C. The loss of lattice water breaks up the regular crystal structure of kaolinite and produces a dehydrated

phase with an amorphous structure, known as Metakaolinite (Equation 1). It is this decrystallization of kaolinite that leads to the disappearance of its XRD patterns. The metakaolinite then transforms to a spinel structure and amorphous silica at a temperature around 800 – 900 °C (Equation 2). Upon further heating up to 1000 °C, recrystallization to form mullite takes place (Equation 3). Similar observations on the thermal properties of kaolinite were reported by other researchers (e.g. Chen et al. 2000; Varga 2007; Ilić et al. 2010).

Thermogravimetric Analysis (TGA) and Differential Scanning Calorimeters (DSC) are the two most commonly used thermoanalytical techniques that have been applied in the investigation of the thermal response of materials. Under a controlled atmosphere with increasing temperature, TGA measures the weight changes in a material as a function of temperature and DSC measures the difference in the amount of heat required to increase the temperature of a sample compared to a reference material. The basic principle underlying DSC is that when the sample undergoes a transformation, such as a phase transition, more or less heat will need to flow into it compared to the reference material to maintain both at the same temperature. Whether less or more heat must flow to the sample depends on whether the process is exothermic or endothermic. By using the two techniques, the changes in the physical and chemical properties of materials that occur with increasing temperature can be identified.

The results obtained from the TGA (plotted as solid black lines) and DSC (plotted as dashed red lines) analyses on the coarse and fine sandstone are shown in Figure 8 (a) and (b), respectively. According to the TGA and DSC curves, the change of the sample property can be divided into three stages for both types of sandstone. In the first stage, when temperature increased from 25 to 400 °C, release of physically adsorbed water in the pores and on the surface of the sample occurs. This process resulted in a slight mass reduction. In the second stage, when temperature increased from 400 to 800 °C, the dehydroxylation of kaolinite takes place. This is indicated by a significant loss of the sample weight and an obvious endothermic peak at about 600 °C. In the third stage, as temperature raised above 800 °C, recrystallization to form mullite occurs. This is indicated by an exothermic peak at about 1000 °C. Comparing the results presented in the two figures, it is clear that a much more significant mass reduction occurred in the fine sandstone (5.07%) than in coarse sandstone (0.76%) as temperature increased from 50 to 1000 °C. The difference is especially significant when the temperature increased from 400 to 800 °C, where the dehydroxylation of kaolinite resulted in a mass reduction of 0.55% for coarse sandstone and 5.07% for fine sandstone.

3.3 Micro-CT results

Figures 9 and 10 show the 2D slice images obtained from coarse and fine sandstone samples, respectively, after being subjected to different temperature treatments. To have a better visual inspection, pores and cracks are marked with red (dark) in the images. The lighter white and grey denote solid mineral grains, most of which is quartz according to the XRD analysis. As shown in Figure 9, coarse grains of the sandstone, which have a size range approximately between 0.5 to 1.0 mm, are cemented by bonding agent (dark grey) between neighbouring particles. At room temperature, it can be observed that the microstructure of the coarse sandstone contains a number of small fissures, both intergranularly and transgranularly. Compared to the coarse sandstone, the fine sandstone has a relatively tight microstructure (Figure 10). Fine grains are arranged in a uniform and compact manner, with micropores and cracks existing between mineral particles. In general, for both types of sandstone samples, the characteristics of the cracking mechanism under increasing heating temperature are similar. The size of pores and cracks does not show obvious change after being subjected to 400 °C. While after 800 °C treatment, it can be seen that pore sizes as well as the porosity of the sample increases significantly. A small number of microcracks develop in certain directions around grain boundaries and contact points. Finally, with the high temperature treatment of 1000 °C, abundant intergranular and intragranular cracks are developed through the sample mass which are closely connected with each other, forming a connected network of cracks.

As mentioned in Section 2.3, image processing was applied to a subset volume of a 3×3×3 mm cube with 600×600×600 voxels. The different steps of the pore network extraction are illustrated in 3D images in Figure 11. The filtered 2D slices were stacked into 3D images of the block sample as shown in Figure 11 (a). Through binarisation, the greyscale images were transferred into binary images with only interior pores in blue and exterior materials in black (Figure 11 (b)). In the next step, as shown in Figure 11 (c), the 3D pore structure of the sample was separated out by volume rendering from the binarised images. Finally, in order to appreciate visually the partitioning quality and more importantly to obtain statistics on the pore space data, pores were separated (represented with different colours) using the "labelling" function in Avizo (Figure 11 (d)). The reconstructed 3D pore structures for fine and coarse sandstone samples after being exposed to different temperature are presented in figures 12 and 13, respectively.

Following the pore labelling step, statistics on the pore quantity and size were calculated, which give a quantitative 3D rock pore structure description. The pore-size distribution frequency histograms for the two samples with different temperature treatment are plotted in figures 14 and 15, respectively. The histograms are plotted with the horizontal axis representing pore volume range in units of "μm^3" and the vertical axis representing porosity. By adding the obtained porosity in different volume ranges, the overall sample porosity was calculated

and shown in the legend of the plot. It should be noted that as the resolution of the 2D slice images was 5 μm, the obtained minimum pore volume is 125 μm^3 and pores with a volume less than 125 μm^3 could not be reconstructed. For coarse sandstone, as shown in Figure 14, the measured total porosity of the sample is 20.05% at room temperature. Pores with a volume less than 10,000,000 μm^3 make up only a small percentage of the total porosity, while the major component of porosity is from large sized interconnected pores that are distributed throughout the sample. Therefore, a secondary axis was used for pore volume range >10,000,000 μm^3; the data in this range are marked with dash outlines. The accumulated porosities of pores with a volume size less than 100,000 μm^3 are similar for samples with different temperature treatment. However, with increasing temperature, an obvious decreasing trend in the porosity can be seen in the range of 100,000 – 10,000,000 μm^3. The most significant porosity change is related to large sized pores which have a volume size >10,000,000 μm^3, where a rapid increase of the accumulated porosity can be observed when the temperature increased from 400 to 1000 °C. This phenomenon can be attributed to the volume expansion of the pores and the connection of small to large sized pores under high temperature.

For fine sandstone, as shown in Figure 15, the pore size distribution shows a main peak in the pore volume range of 125-1,000 μm^3 at room temperature (contributing about 69% of the overall sample porosity). After 400 °C treatment, there is a slight decrease in the quantity of fine pores (125-1,000 μm^3), whilst there is an increase in the accumulated porosity of larger sized pores (1,000 – 1,000,000 μm^3). The alteration of the fine pores to larger sized pores at 400 °C leads to a slight overall porosity increase from 2.28% to 2.81%. After 800°C treatment, more significant changes take place in the sample microstructure, demonstrated by the increase of the accumulated porosity in the pore volume range of 1,000 – 1,000,000 μm^3. Also, large sized pores with a volume larger than 1,000,000 μm^3 were created. The overall porosity of the sample was nearly 1.9 times higher than that at 400 °C. This change in the sample porosity can be attributed to the phase transformation and partial melting of the minerals contained within the sandstone (Zhang et al. 2005; Wu et al. 2013). With the high temperature treatment of 1000 °C, the accumulated porosity appears to be increased significantly in all the pore volume ranges with a peak in the range of 1,000-10,000 μm^3. This change can be attributed to the propagation of existing cracks and the formation of new microcracks in the sample.

4. Discussion

The strength of rock depends on a number of factors, such as mineralogical composition; textural and microstructural characteristics, including void space, water content, grain size, shape and arrangement; microcrack distribution and fracture mechanism; the strength of the mineral constituents and the nature of the bonding between them. In a similar manner to strength, the elastic response of rock depends mainly on the elastic properties of the constituent minerals, the degree of cementation and porosity (Sygała et al. 2013). Under the influence of high temperatures, another important factor that affects rock strength and elastic response is the thermal expansion of the constituent minerals. At high temperatures, varying thermal expansion characteristics within different mineral grains causes thermal stresses in the mineral structure to increase, potentially leading to the fracture of individual mineral grains and expansion of inner cracks, which may further lead to disaggregation of the rock (Huotari and Kukkonen 2004; Wan et al. 2009; Zhang et al. 2014). In addition to structural deformation induced by mineral expansion, other factors which may lead to alteration of the rock internal structure include dehydration, decomposition, melting, and phase-change reactions (Zhang et al. 2005; Tian et al. 2012; Wu et al. 2013).

The data presented indicates that high temperatures have a significant effect on the mechanical properties of sandstone. The changes due to heating can be divided into three stages. First, for temperatures up to 400 °C, physically adsorbed water within the pores is evaporated and gases contained within the inner structure of the rock are emitted. This reduction of moisture content (for a given volume) has been shown to have a positive impact on rock strength (Erguler and Ulusay 2009) due to the additional void space available to allow compaction. For both coarse and fine sandstone, the pores and microcracks become smaller under axial compression, especially after the onset of plastic yield. Thus, the combined action of thermal evaporation and axial compression increases the density of the rock and its ability to resist deformation.

In the second stage, for temperatures in the range of 400 to 800 °C, the sandstone constituent mineral kaolinite loses its constitutional water and begins decomposing (at about 600 °C). The loss of lattice water breaks up the regular crystal structure of kaolinite and produces a dehydrated phase known as metakaolinite, which can be considered as a semi-crystalline mineral with amorphous structure (Ilić et al. 2010). A significant reduction of mass, increase in volume, and increase in porosity is associated with this phase transformation, resulting in a rise is the porosity of the rock. Further heating to 800 °C initiates the formation and development of microcracks in the structure of sandstone. However, extensive propagation and coalescence of microcracks does not yet take place in the rock mass. The stiffness of the sandstone under axial compression decreases as a result of the increased porosity. Similar to the compression mechanism observed in the first stage,

a temporary increase or a maintaining of the rock strength can be attributed to the reduced sliding between particles under axial loading. Fine sandstones exhibits more significant strength increase and stiffness reduction than coarse sandstones after 800 °C treatment. This behaviour can be attributed to the structural characteristics of the two types of samples. Comparing with fine-grained sandstone, the higher porosity of the coarse-grained sandstone reduces the potential of cracking due to expansion of minerals. Therefore, the effect of thermal treatment is comparatively less significant in coarse sandstones.

In the third stage, when temperature rises above 800 °C, the mineral composition of sandstone becomes unstable. Anisotropic deformations take place due to differing thermal expansion coefficients of constituent minerals, depending on the crystallographic orientation of the minerals (Huotari and Kukkonen 2004). This results in stress concentrations at grain boundaries and contact points. New microcracks develop when thermal stresses exceed the material strength. Melting and thermal decomposition may also occur and contribute to the development of microcracks. Upon further heating, networks of microcracks propagate and grow; intragranular cracks and propagation of intergranular cracks may lead to fracturing of individual mineral grains, which may further lead to obvious disaggregation of the rock structure. Under loading, extensive microcracks propagate rapidly along different directions through the sample mass, leading to a significant reduction of the strength and stiffness. On account of more significant propagation and coalescence of microcracks, the strength of fine sandstone was reduced more than that of coarse sandstone after being heated to a temperature of 1000 °C.

5. Conclusions

This paper presented data from micro-CT scanning and traditional rock mechanics tests performed on sandstone samples treated at a range of temperatures between 20 and 1000 °C. Multistage triaxial tests were used to determine the mechanical properties of the samples. XRD and thermal analyses were performed as supplementary methods to better understand the physical and chemical changes of the sandstone under increasing temperature. Micro-CT analyses were carried out on selected samples in order to reveal the microstructural changes that take place as a result of the heating process. 3D characterization of the sample porosity and pore size distribution were performed in a manner of quantitative comparison between samples with different temperature treatment. The relationship between micro-structure and macro-mechanical characteristics of sandstone at high temperature was then discussed. The results obtained from the investigations suggest that the mechanical property changes of sandstone with increasing temperature is closely related to its physical and chemical changes which can be divided into three stages:

- In the first stage, from room temperature to 400 °C, physically adsorbed water within pores is evaporated and gases contained in the inner structure of the rock are emitted. The combined action of thermal evaporation and axial compression increases the density of the rock and its ability to resist deformation under axial compression. This results in an increase in strength and reduction of stiffness of the rock.
- The second stage from 400 to 800 °C involves the most significant processes that change the physical and mechanical properties of sandstone. Decrystallization of kaolinite and the formation of metakaolinite take place at a temperature around 600 °C, resulting in a significant reduction of mass and increase in volume and porosity. Heating to 800 °C causes the formation and development of microcracks due to thermal expansion of the constituent minerals. The stiffness of the sandstone under axial compression decreases as a consequence of increased porosity. The increased porosity exhibited a positive impact on the rock strength, possibly caused by reduced sliding between particles under compression.

- In the third stage, for temperatures above 800 °C, the mineral composition of sandstone becomes unstable. Variation of thermal expansion coefficients of constituent minerals results in stress concentrations at grain boundaries and contact points. Melting and thermal decomposition of the constituent minerals also takes place. The development of both intragranular and intergranular cracks and the formation of crack networks lead to breakage of the rock structure, resulting in a significant reduction of the rock strength and elastic modulus under applied loading.

This study demonstrates the suitability of applying the computed micro-tomography technique to provide detailed non-destructive characterization of the three-dimensional rock fabric. Statistical analysis of porosity and pore size distribution was achieved by analysing the 3D images. The characterization provides valuable data for the understanding of complex cracking mechanisms and void network evolutions that take place in the rock microstructure under increasing temperature. The insight into the true spatial arrangements of the rock fabric makes it possible to track the correspondence between the micro-structure and macro-mechanical characteristics of rocks. It can be concluded that X-ray micro-tomographic scanning coupled with image analysis techniques has significant potential to become a common tool and powerful approach to be applied in geosciences.

Acknowledgments

References

ASTM (American Society for Testing and Materials). Standard guide for computed tomography (CT) imaging, ASTM designation E 1441–92a, in 1992 annual book of ASTM standards, section 3 metals test methods and analytical procedures: Philadelphia, ASTM, **1992**, 690–713.

Brown, E.T. Rock characterization, testing and monitoring, ISRM suggested methods. Pergamon Press, Oxford, **1981**, 107–127.

Brotóns, V.; Tomás, R.; Ivorra, S.; Alarcón, J. C. Temperature influence on the physical and mechanical properties of a porous rock: San Julian's calcarenite. *Engineering Geology*. **2013**, *167(4)*, 117-127.

Bloomfield, J.; Gooddy, D.; Bright, M.; Williams, P. Pore-throat size distributions in Permo-Triassic sandstones from the United Kingdom and some implications for contaminant hydrogeology. *Hydrogeology Journal*. **2001**, 9(3), 219-230.

Chen, C. Y.; Lan, G. S.; Tuan, W. H. Microstructural evolution of mullite during the sintering of kaolin powder compacts. Ceramics international. **2000**, 26(7), 715-720.

Chen Y-L.; Ni J.; Shao W.; Azzam R. An experimental study on the influence of temperature on the mechanical proper-ties of granite under a uni-axial compression and fatigue loading. *International Journal of Rock Mechanics & Mining Sciences*. **2012**, *56(15)*, 62–66.

Erguler, Z. A.; Ulusay, R. Water-induced variations in mechanical properties of clay-bearing rocks. *International Journal of Rock Mechanics and Mining Sciences*. **2009**, 46(2), 355-370.

Huotari, T.; Kukkonen, I. Thermal expansion properties of rocks: Literature survey and estimation of thermal expansion coefficient for Olkiluoto mica gneiss. *Posiva Oy, Olkiluoto, Working Report*, **2004**, 4, 62.

Heuze, F. E. High-temperature mechanical, physical and thermal properties of granitic rocks—a review. *International Journal of Rock Mechanics and Mining Sciences & Geomechanics Abstracts*. **1983**, *20(1)*:3-10.

Ilić, B. R.; Mitrović, A. A.; Miličić, L. R. Thermal treatment of kaolin clay to obtain metakaolin. *Hemijska industrija*. **2010**, 64(4), 351-356.

Liu, J. R.; Mao, X.; Zhang, L.; Ma, D. Thermal properties of mudstone at high temperature. *International Journal of Geomechanics*. **2013**, *14(5)*, 04014023.

Liu, J. R.; Wu, X. D. Microscopic experiment of thermal treated rock. *Journal of Southwest Petroleum University (Science & Technology Edition)*. **2008**, 29*(4)*, 006.

Mao, X. B.; Zhang, L. Y.; Li, T. Z.; Liu, H. S. Properties of failure mode and thermal damage for limestone at high temperature. *Mining Science and Technology (China)*. **2009**, *19(3)*, 290-294.

Peng, S.; Hu, Q.; Dultz, S.; Zhang, M. Using X-ray computed tomography in pore structure characterization for a Berea sandstone: resolution effect. *Journal of Hydrology*, **2012**, 472-473(4), 254-261.

Ranjith, P. G.; Viete, D. R.; Chen, B. J.; Perera, M. S. A. Transformation plasticity and the effect of temperature on the mechanical behaviour of Hawkesbury sandstone at atmospheric pressure. *Engineering Geology*, **2012**, *151(151)*, 120-127.

Rao, Q. H.; Wang, Z.; Xie, H. F.; Xie, Q. Experimental study of mechanical properties of sandstone at high temperature. *Journal of Central South University of Technology, China*. **2007**, *14(1)*, 478-483.

Stefaniuk D, Tankiewicz M, Stróżyk J (2014) X-Ray Microtomography (ìCT) as a useful tool for visualization and interpretation of shear strength test results. Studia Geotechnica et Mechanica XXXVI(4): 163-171.

Stesky, R. M.; Brace, W. F.; Riley, D. K.; Robin, P. Y. Friction in faulted rock at high temperature and pressure. *Tectonophysics*. **1974**, *23(1)*, 177-203.

Sygała, A.; Bukowska, M.; Janoszek, T. High temperature versus geomechanical parameters of selected rocks–the present state of research. *Journal of Sustainable Mining*, **2013**. *12(4):45-51*.

Tian, H.; Kempka, T.; Xu, N. X.; Ziegler, M. Physical properties of sandstones after high temperature treatment. Rock mechanics and rock engineering, **2012**, 45(6), 1113-1117.

Varga, G. The structure of kaolinite and metakaolinite. *Epitoanyag*, **2007**, *59(1)*, 6-9.

Vollbrecht, A.; Rust, S.; Weber, K. Development of microcracks in granites during cooling and uplift: examples from the Variscan basement in NE Bavaria. *Germany. Journal of Structural Geology,* **1991**, *13(7)*, 787-799.

Wan, Z. J.; Zhao, Y. S.; Zhang, Y.; Wang, C.. Research status quo and prospection of mechanical characteristics of rock under high temperature and high pressure. *Procedia Earth and Planetary Science*. **2009**, *1(1)*, 565-570.

Wu, G.; Wang, Y.; Swift, G.; Chen, J. Laboratory investigation of the effects of temperature on the mechanical properties of sandstone. *Geotechnical and Geological Engineering*. **2013**, *31(2)*, 809-816.

Zhang, L.; Mao, X.; Lu, A. Experimental study on the mechanical properties of rocks at high temperature. *Science in China Series E: Technological Sciences*. **2009**, *52(3)*, 641-646.

Zhang, L.; Mao, X.; Liu, R.; Guo, X.; Ma, D. The mechanical properties of mudstone at high temperatures: an experimental study. Rock mechanics and rock engineering. **2014**, *47(4)*, 1479-1484.

Zhang, Y.; Zhang, X.; Zhao, Y. S. Process of sandstone thermal cracking. *Chinese Journal of Geophysics*. **2005**, *48(3)*, 722-726.

Zhang, Y.; Wan, Z. J.; Zhao, Y. S. Meso-experiment of fine sandstone thermal crack laws. *J Liaoning Tech Univ*. **2007**, *26(4)*, 529-531.

Notation

The following is a list of symbols used in this paper:

E = Young's Modulus
Θ = Angle of diffraction

Table 1. Details of intact cores							
Sample Ref.	Temp. Treat. (°C)	Volume (cm³)	Volume change (%)	Mass (g)	Mass change (%)	Density (g/cm³)	Density change (%)
CS-A	20	81.04	/	192.6	/	2.38	/
CS-F	20	80.46	/	181.31	/	2.25	/
FS-P	20	80.24	/	203.18	/	2.53	/
FS-R	20	83.77	/	211.76	/	2.53	/
CS-I	20	80.47	0	190	-0.07	2.36	-0.07
	400	80.47		189.87		2.36	
CS-J	20	79.86	0.08	189.69	-0.08	2.37	-0.16
	400	79.92		189.53		2.37	
FS-O	20	80.34	0.06	210.4	-0.07	2.62	-0.13
	400	80.39		210.25		2.62	
FS-Q	20	80.70	0.05	203.21	-0.04	2.52	-0.90
	400	81.14		202.48		2.50	
CS-B	20	80.75	1.98	187.32	-1.99	2.32	-3.90
	800	82.35		183.59		2.23	
CS-C	20	80.66	2.21	187.33	-2.00	2.32	-4.11
	800	82.44		183.59		2.23	
FS-K	20	80.17	3.08	208.73	-6.76	2.60	-9.55
	800	82.64		194.62		2.36	
FS-L	20	80.27	3.41	205.65	-5.00	2.56	-8.14
	800	83.01		195.36		2.35	
CS-D	20	80.52	2.96	187.29	-2.16	2.33	-4.97
	1000	82.90		183.25		2.21	
CS-E	20	80.64	3.19	185.32	-1.94	2.30	-4.97
	1000	83.21		181.72		2.18	
FS-M	20	80.18	2.52	209.23	-5.62	2.61	-7.93
	1000	82.20		197.48		2.40	
FS-N	20	80.10	4.38	208.51	-5.32	2.60	-9.30
	1000	83.61		197.41		2.36	

"CS" Coarse Sandstone; "FS": fine sandstone; "+": increase; "-": decrease

Figure 1 Laboratory prepared intact core samples (top: coarse sandstone; below: fine sandstone)
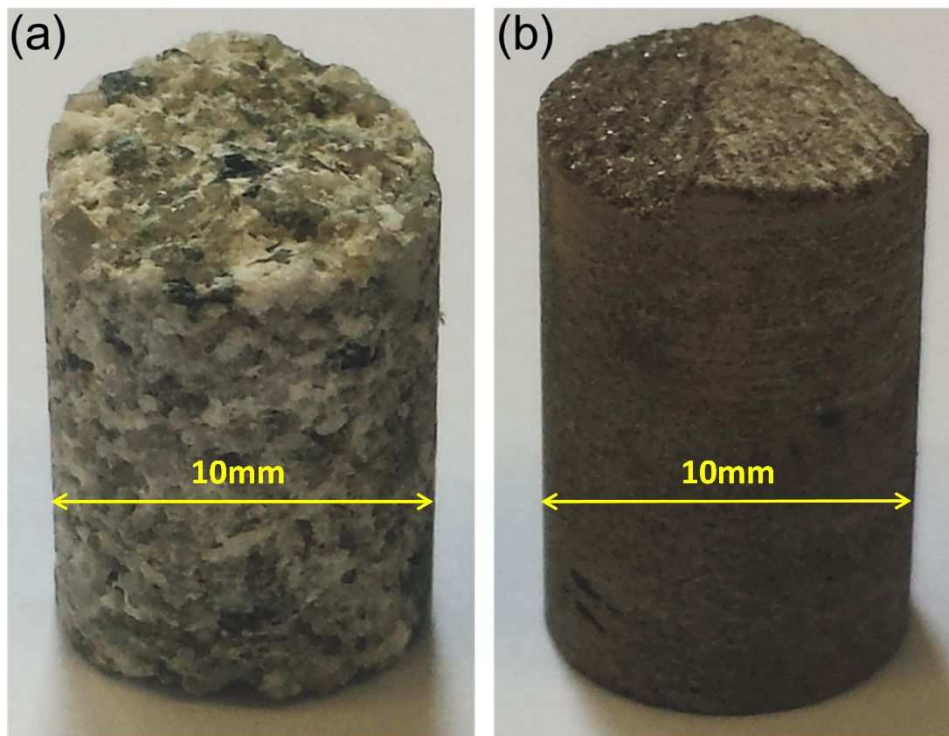
Figure 2 (a) Coarse sandstone and (b) fine sandstone samples prepared for CT scanning
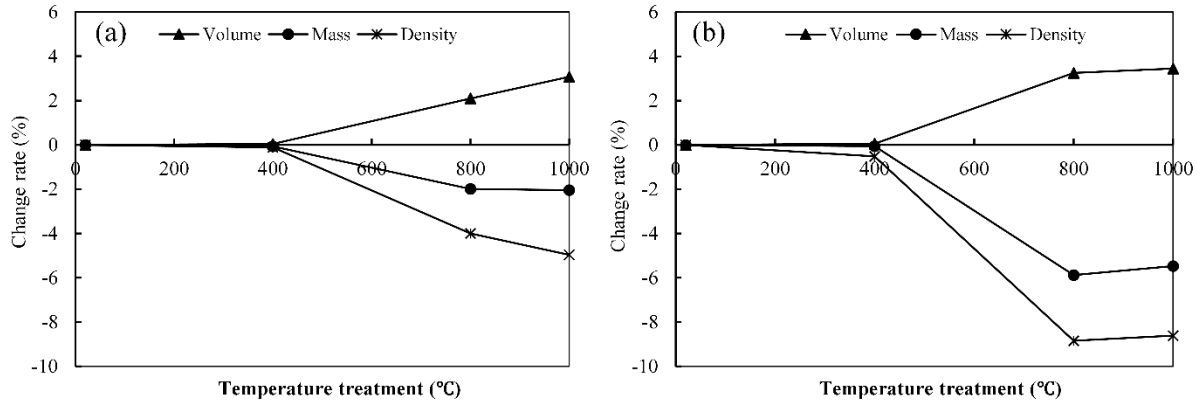
Figure 3 Volume, mass and density changes for (a) Coarse sandstone and (b) fine sandstone, after different temperature treatment
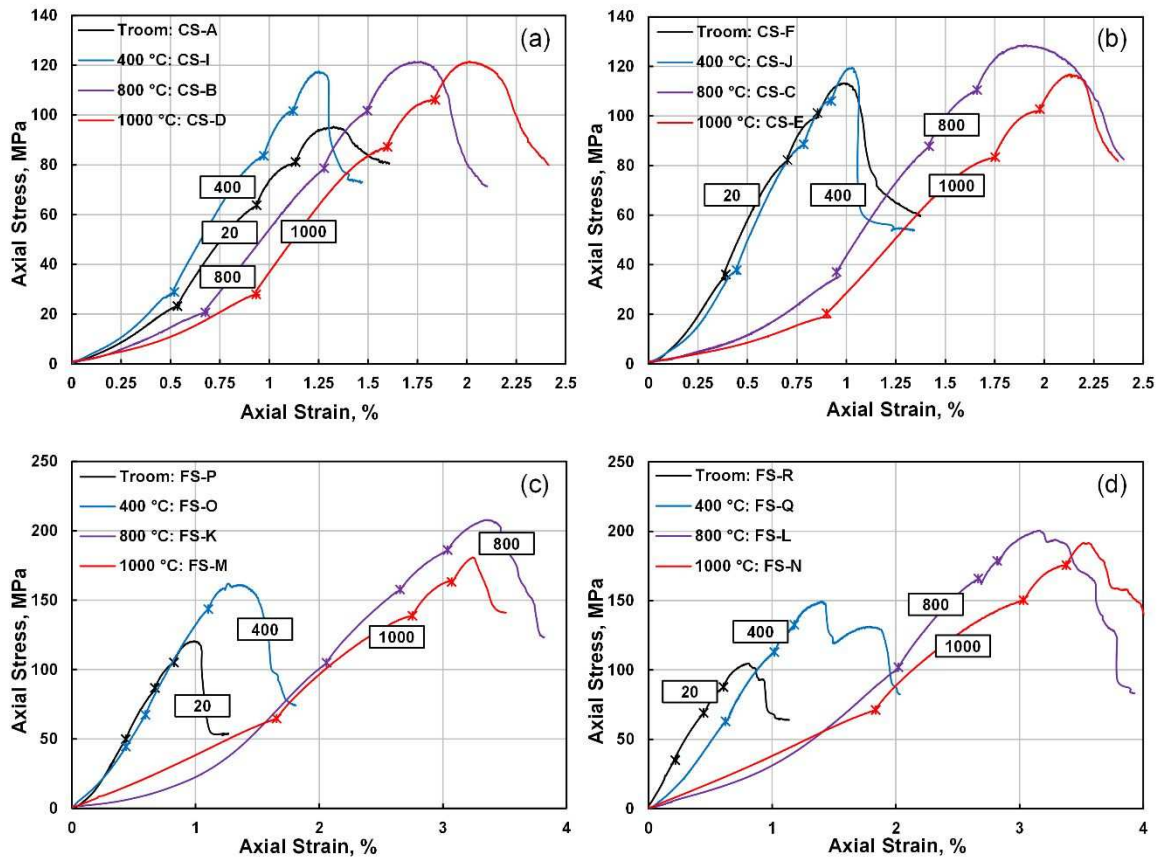

Figure 4 Stress-strain curves obtained from multistage triaxial tests for: (a), (b) coarse sandstone and (c), (d) fine sandstone
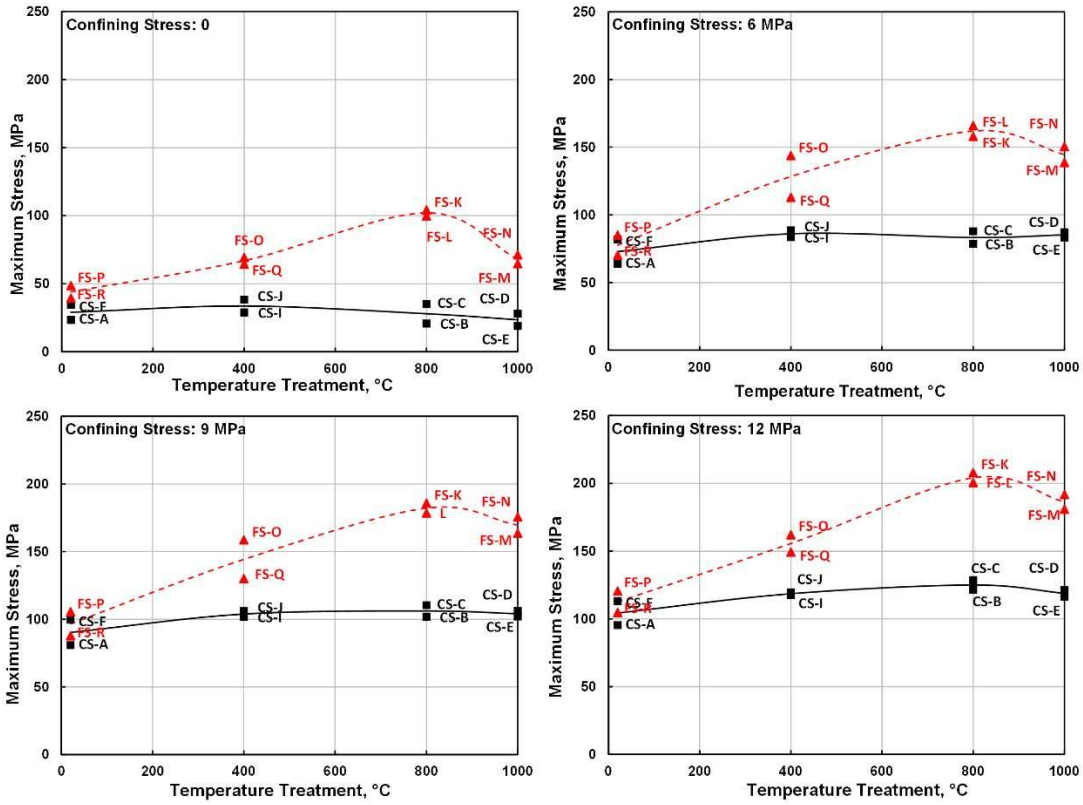
Figure 5 Peak stress obtained at different confining stress levels for coarse and fine sandstone samples
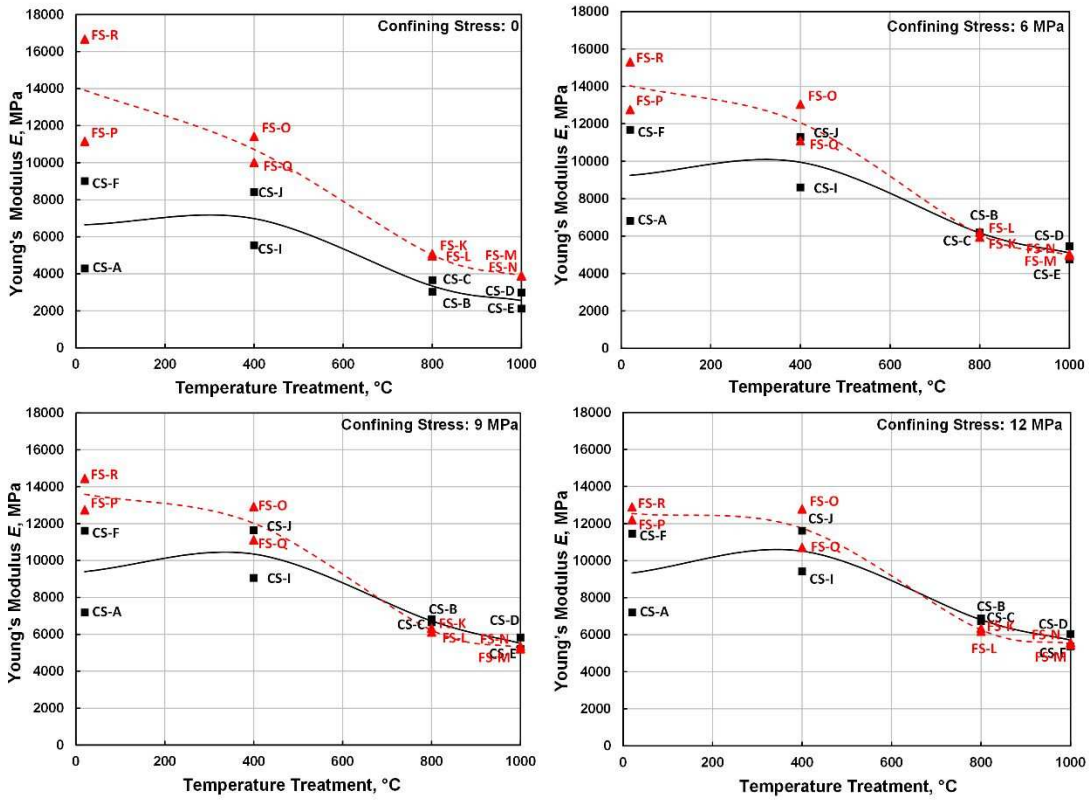
Figure 6 Secant Young's modulus at different confining stress levels for coarse and fine sandstone
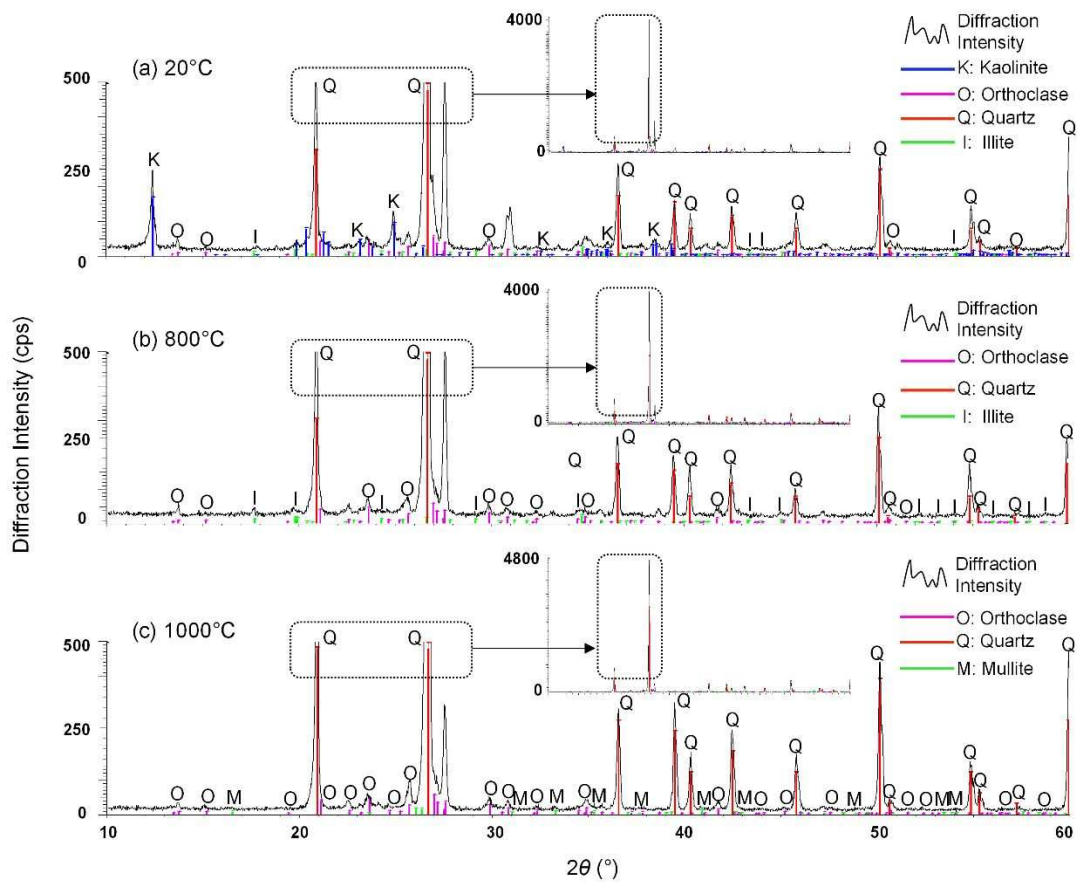
Figure 7 XRD results on sandstone samples with different temperature treatment: (a) 20 °C; (b) 800 °C and (c) 1000 °C
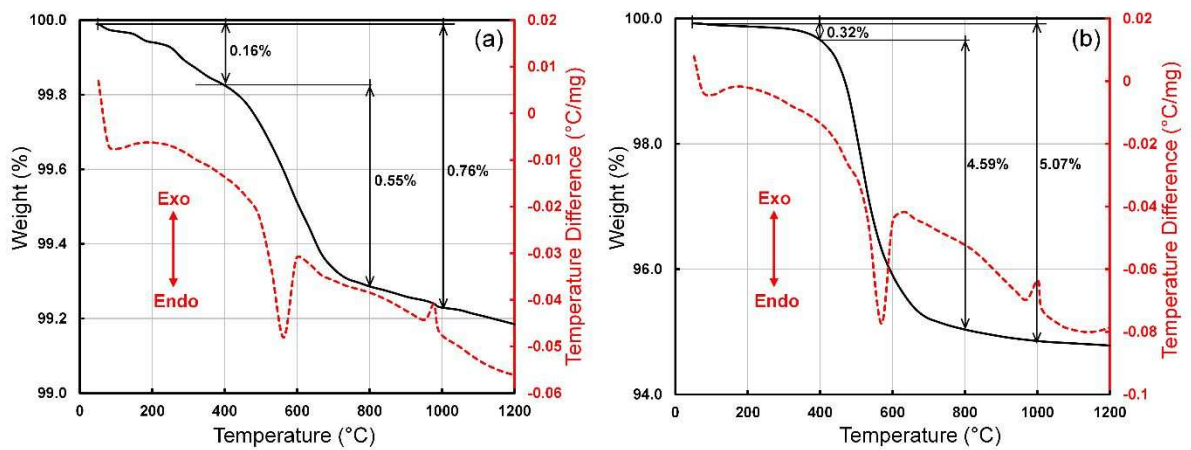
Figure 8 Results obtained from TGA (black solid) and DSC (red dashed) analyses on: (a) coarse sandstone and (b) fine sandstone
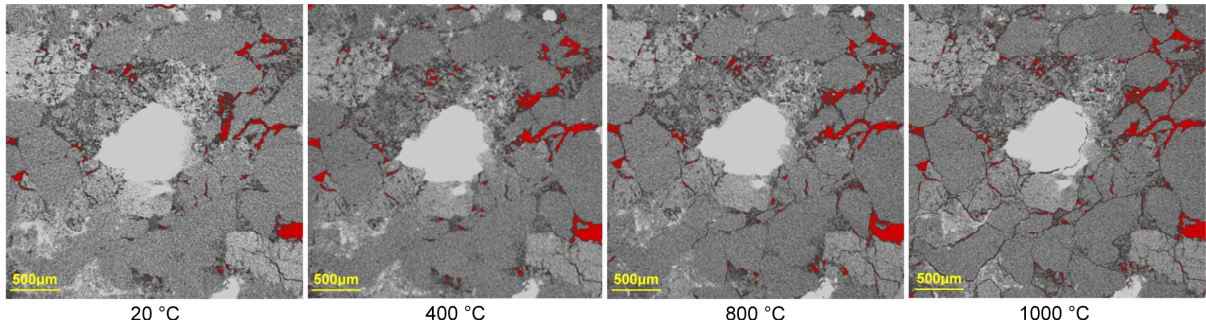
Figure 9 2D slice images (3×3 mm) with resolution of 5 μm obtained from coarse sandstone sample after different temperature treatment
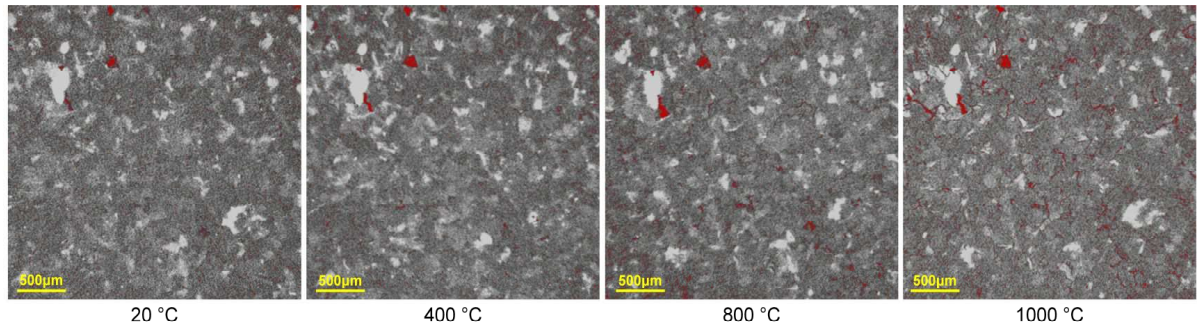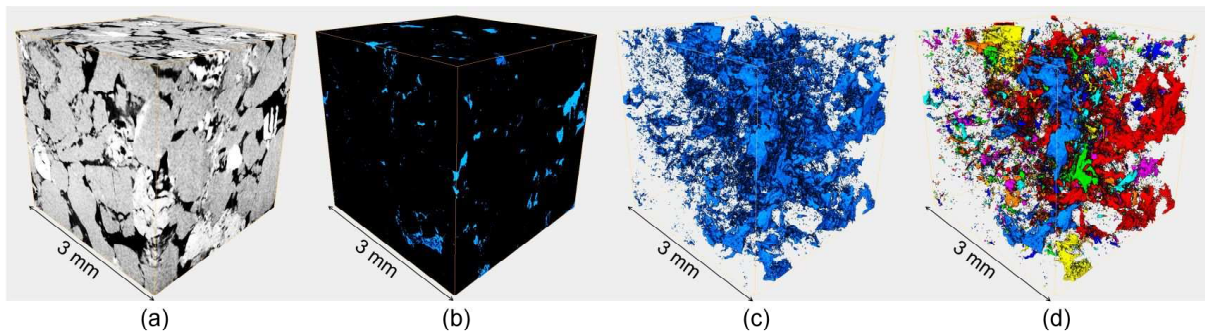

Figure 10 2D slice images (3×3 mm) with resolution of 5 μm obtained from fine sandstone sample after different temperature treatment

Figure 11 Four main steps of acquisition of 3D rock pore structure: (a) acquisition of a 3D block; (b) isolating the porosity by binarisation; (c) volume rendering of pores from the binarised images; (d) labelled image of pore structure
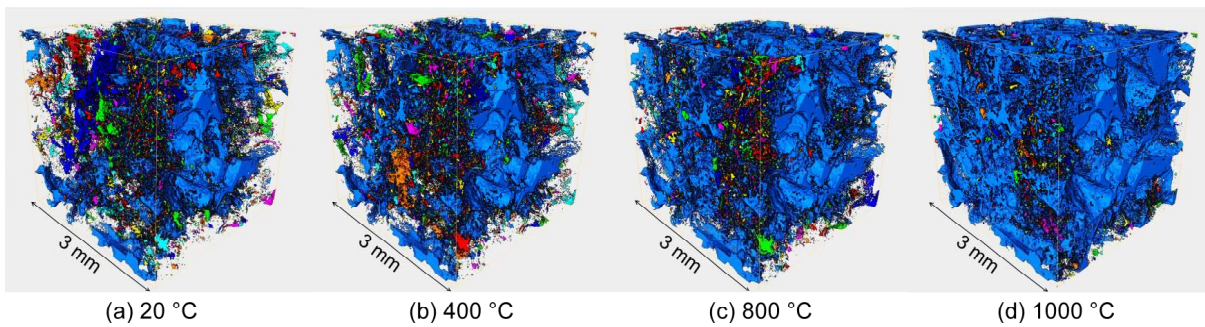
Figure 12 Reconstructed 3D pore structure (3×3×3 mm) for coarse sandstone sample after different temperature treatment

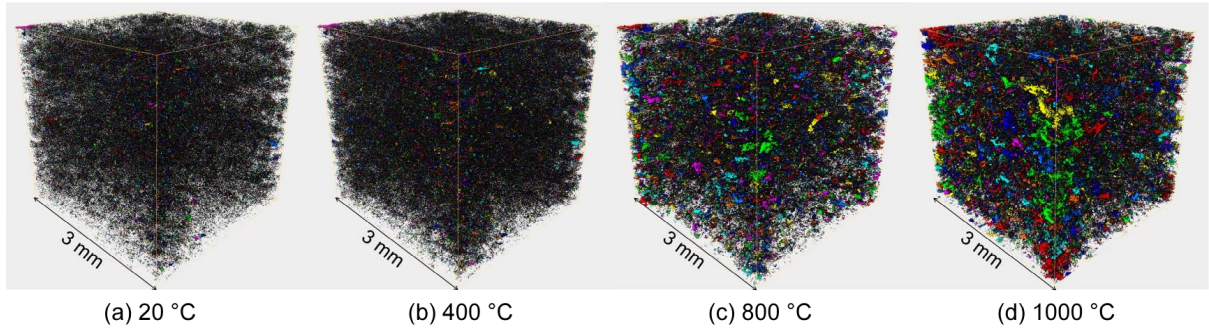(a) 20 °C   (b) 400 °C   (c) 800 °C   (d) 1000 °C

Figure 13 Reconstructed 3D pore structure (3×3×3 mm) for fine sandstone sample after different temperature treatment
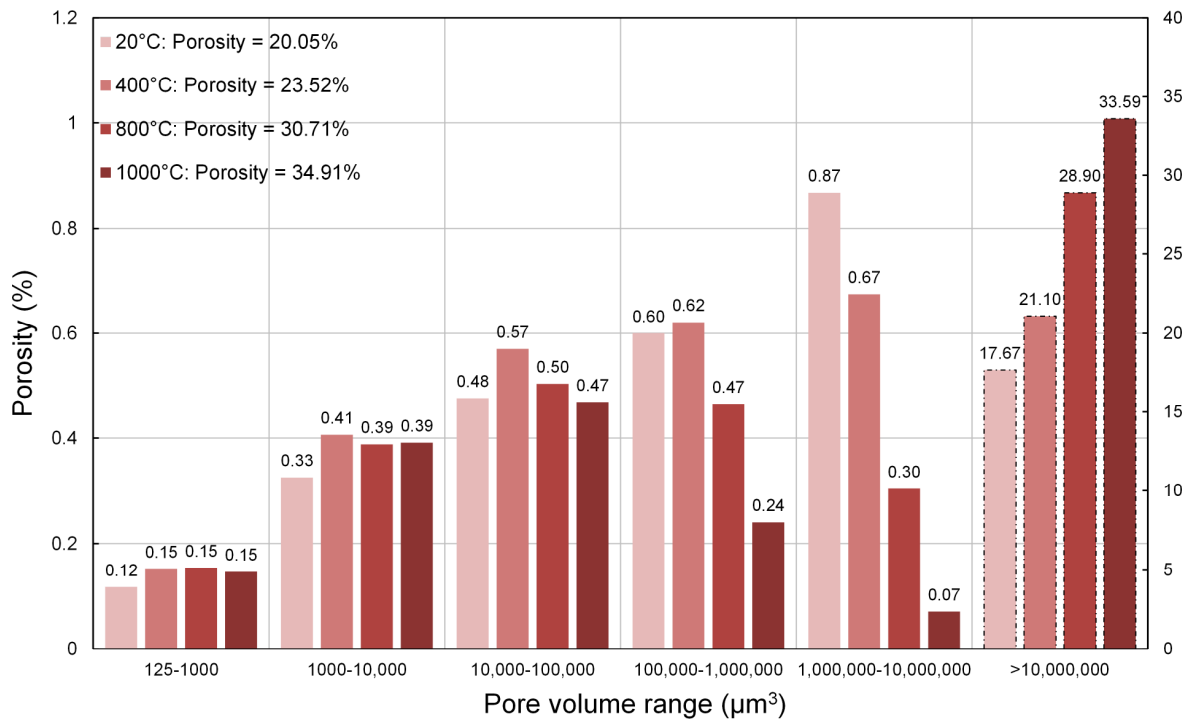

Figure 14 Pore-size distribution frequency histogram for coarse sandstone sample after being subjected to different temperatures
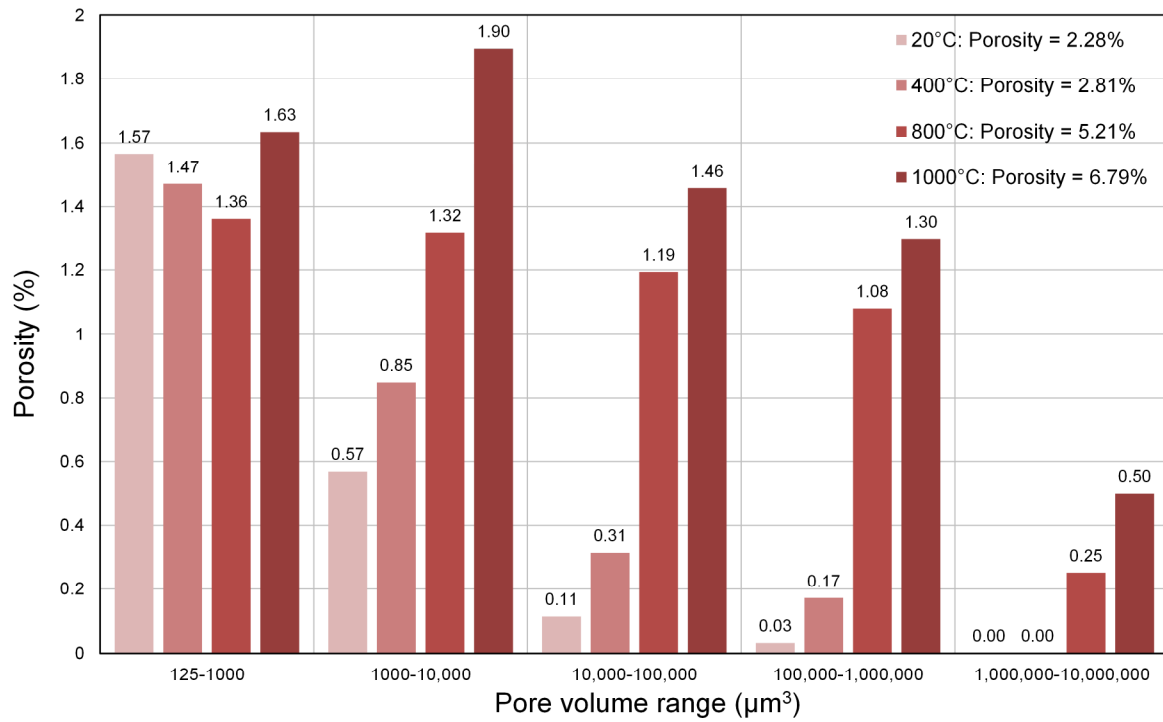
Figure 15 Pore-size distribution frequency histogram for fine sandstone sample after being subjected to different temperatures